Highlights from CMS

Available online at www.sciencedirect.com

SciVerse ScienceDirect

Nuclear Physics A 904–905 (2013) 43c–50c

NUCLEAR PHYSICS A

www.elsevier.com/locate/nuclphysa

Highlights from CMS

Gunther Roland (for the CMS Collaboration)[1]

Massachusetts Institute of Technology, Cambridge, MA, USA

Abstract

The CMS collaboration has used a data set of 1 billion PbPb collisions at the LHC to study the behavior of strongly interacting matter at high temperature. In this Paper, we present selected recent highlights from this effort, with a particular emphasis on results related to the hydrodynamic expansion of the produced matter, the energy loss of partons and the dissociation of quarkonia.

1. Introduction

In 2011, the Compact Muon Solenoid (CMS) experiment [1] at the Large Hadron Collider (LHC) collected a sample of PbPb collisions at $\sqrt{s_{NN}} = 2.76$ TeV, corresponding to an integrated luminosity of 150 μb^{-1}. For data-taking, CMS employed a set of sophisticated trigger algorithms, resulting in high statistics samples of high momentum jets, photons, single tracks, single muons and dimuons, and a complete sample of the 0.2% most central collisions. In this Paper, an overview of results obtained using these triggered samples is provided. The results illustrate the power and versatility of the CMS apparatus, allowing significantly increased kinematic reach for some measurements, like e.g. anisotropy measurements at p_T up to 60 GeV/c, and enabling several new measurements, like the first studies of photon-jet correlations and b-tagged jets in heavy-ion collisions. A collection of all submitted CMS heavy-ion publications, as well as documentation of all preliminary results, can be found at [2].

2. Hydrodynamic flow in ultra-central collisions

One of the key difficulties in the quantitative extraction of medium transport coefficients in studies of anisotropic flow stems from uncertainties in the description of the initial state geometry. The recent focus on higher order flow components, in particular triangular flow [3], has provided new handles to reduce some of these uncertainties. A complementary approach is provided by studies of ultra-central collisions, where the initial state eccentricities are provided purely by fluctuations in the participant geometry. Fig. 1(left) shows ϵ_n calculated using a Glauber MC model for $n = 1$–7. For completely overlapping nuclei ($b = 0$), all ϵ_n for $n > 1$ converge to the same value. Therefore ultra-central collisions provide a particularly well defined starting point for studies of the relative magnitude of final state flow harmonics, v_n and the extraction of the shear viscosity to entropy density ratio, η/s.

[1] A list of members of the CMS Collaboration and acknowledgments can be found at the end of this issue.

0375-9474/
http://dx.doi.org/10.1016/j.nuclphysa.2013.01.043

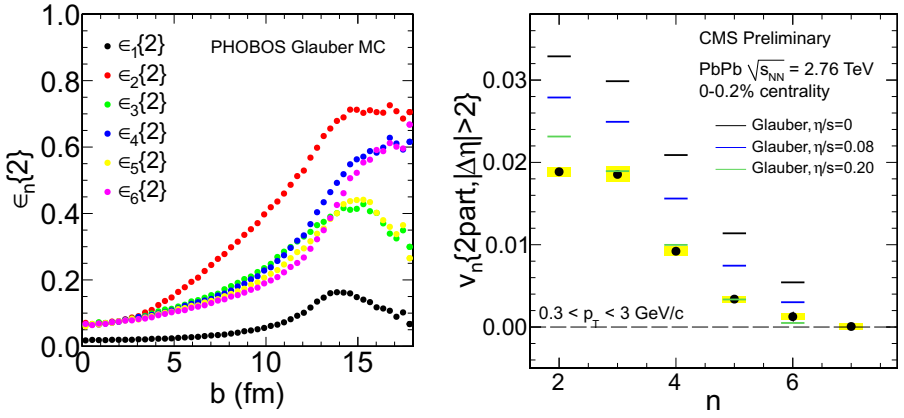

Figure 1: (Left): The eccentricities, ϵ_n, calculated as a function of impact parameter, b, in a Glauber MC model for PbPb collisions at 2.76TeV. 0-0.2%, 0–1% and 0-2.5% centrality ranges correspond to b ranges of 0-0.7 fm, 0-1.6 fm and 0-2.5 fm. (Right): Comparison of p_T-integrated (0.3–3.0 GeV/c) v_n data with viscous hydrodynamic calculations from Ref. [4] for different η/s values, in 0-0.2% central PbPb collisions at $\sqrt{s_{NN}}$ = 2.76 TeV. Error bars denote the statistical uncertainties of the data, while the grey bands correspond to the systematic uncertainties.

To approximate the ideal $b = 0$ case as much as experimentally possible, CMS performed an analysis of flow coefficients for the 0.2% most central PbPb collisions at $\sqrt{s_{NN}}$ = 2.76 TeV. The results are shown in Fig. 1(right) for the p_T-integrated v_2–v_6 over $0.3 < p_T < 3$ GeV/c and are compared with calculations from M. Luzum and J. Y. Ollitrault using viscous relativistic hydrodynamics [4]. Lines with different colors correspond to calculations with different values of η/s ranging from 0 to 0.2. An η/s value of approximately 0.2 is favored by this comparison, although v_2 seems to be over-predicted.

Similarly, comparisons to calculations by C. Shen, Z. Qiu and U. Heinz using event-by-event 2+1D viscous hydrodynamics (VISH2+1D) suggest that the η/s is within the range of 0.08–0.2, although again some tension between the best description of v_2 and higher order flow components is observed.

3. Path-length dependent jet-quenching and v_2 at high p_T

Large uncertainties remain on some of the key properties of the parton energy loss process, such as the detailed path-length dependence. Constraints on these properties can be improved by requiring models to describe complementary measurements simultaneously, such as the centrality dependence of both the single hadron suppression and the azimuthal anisotropy of particles at high p_T [5, 6]. The high-p_T anisotropy can be characterized by the second-order Fourier coefficient (v_2) of the azimuthal particle distribution, which directly reflects the differential path-length dependent energy loss.

Figure 2 shows that as a function of particle p_T, v_2 exhibits a rapid rise, with a maximum at $p_T \approx 3$ GeV/c, followed by a rapid decrease for p_T values up to about 10 GeV/c and a slow decrease for $p_T > 10$ GeV/c. The anisotropy remains larger than zero up to at least $p_T \approx 40$ GeV/c. These results extend previous measurements to a much larger p_T regime, where

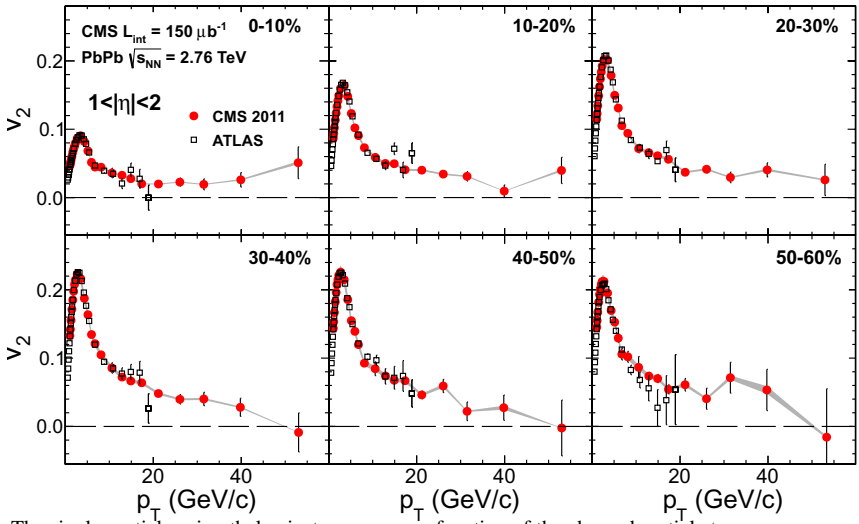

Figure 2: The single-particle azimuthal anisotropy, v_2, as a function of the charged particle transverse momentum from 1 to 60 GeV/c with $|\eta| < 1$ for six centrality ranges in PbPb collisions at $\sqrt{s_{NN}}$ = 2.76 TeV, measured by the CMS experiment (solid markers). Error bars denote the statistical uncertainties, while the grey bands correspond to the small systematic uncertainties. Comparison to results from the ATLAS (open squares) and CMS (open circles) experiments using data collected in 2010 are also shown.

particle production is dominated by parton fragmentation and where the anisotropy is attributable to path-length differential energy-loss model. This is supported by measurements of v_3 vs. p_T [7], showing that v_3 drops to zero much faster than v_2, as expected in a path-length dependence picture.

4. Jet quenching and nuclear modification factors

The nuclear modification factor R_{AA} defined as the ratio of particle yields (normalized by the nuclear overlap T_{AA}) in nucleus-nucleus compared to nucleon-nucleon collisions, remains one of the key observables in studies of jet quenching more than a decade after the first observation of this effect at RHIC.

CMS has obtained R_{AA} for a large variety of single particles as well as jets. New R_{AA} measurements presented at this meeting included updated measurements for photons, Z^0 bosons, and B-mesons (via $B \to J/\psi$ decays), the first CMS measurement of W-boson R_{AA} and inclusive jet R_{AA} and the first measurement of b-tagged jets in heavy-ion collisions. The jet R_{AA} measurements will be discussed below.

Figure 3 shows the unfolded jet R_{AA}, using Bayesian unfolding. The uncertainties shown are uncorrelated (thin vertical line) and total statistical uncertainty (thicker magenta vertical box), as well as the systematic uncertainty (grey band). In addition, an overall scale uncertainty is shown with a green box. For the most peripheral PbPb collisions, the nuclear modification factor is near unity. R_{AA} decreases to about 0.5 for central collisions. For all centrality selections, the jet R_{AA} is approximately flat as a function of p_T over the range studied. The jet suppression seen in central collisions shows good consistency with the results for single charged hadrons, where a suppression factor of 0.5 for $35 < p_T < 40$ GeV/c is seen.

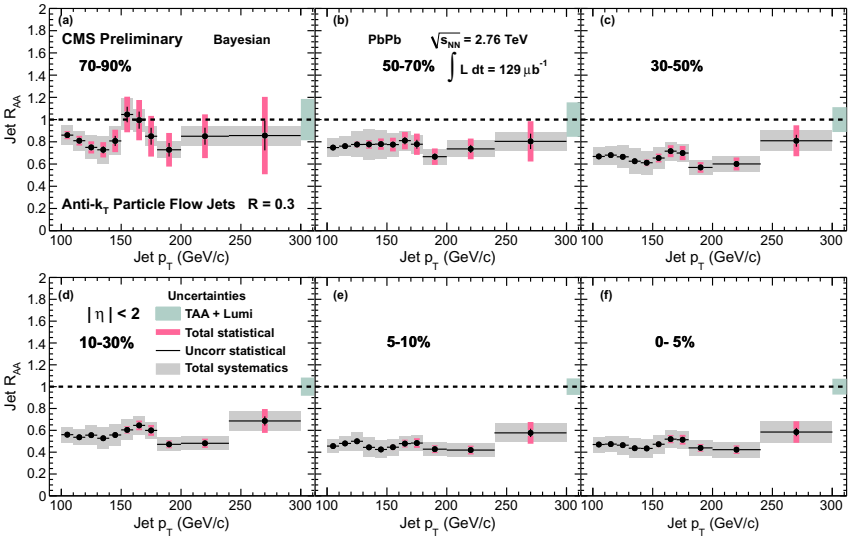

Figure 3: Bayesian unfolded jet R_{AA} for jets found with the anti-k_{T} algorithm (R=0.3). Vertical lines represent the uncorrelated statistical uncertainty, thin magenta vertical bands the total statistical uncertainty, and the wide grey bands represent the systematic uncertainty. The common uncertainties from T_{AA} and luminosities are shown as a green box above 300 GeV/c.

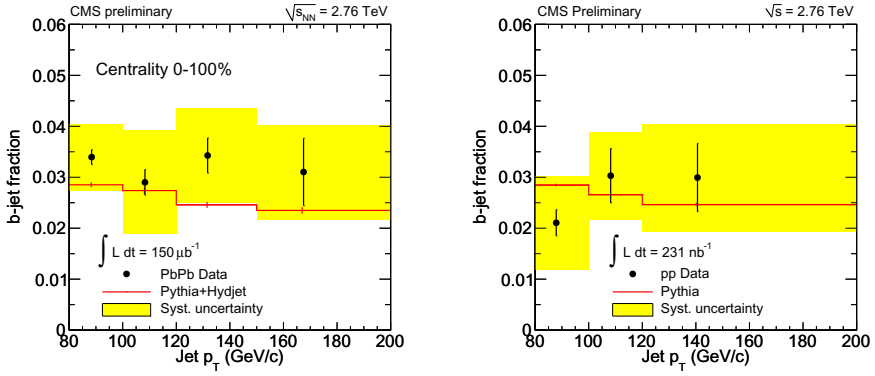

Figure 4: The b-jet to inclusive jet ratio in 0-100% PbPb collisions (left) and pp collisions (right) as a function of jet p_{T} compared to PYTHIA embedded in HYDJET (PbPb) and PYTHIA (pp). Data and MC have not been corrected for bin migration effects from finite jet resolution.

Recent CMS data have shown that non-prompt J/ψ originating from decays of B mesons are suppressed in PbPb collisions with respect to the pp expectation [8]. At high p_{T}, a more direct measurement of b-quark energy loss can be performed using fully reconstructed jets in combination with b-tagging techniques developed for pp collisions.

Heavy flavor jets can be tagged by the presence of displaced vertices, allowing the definition

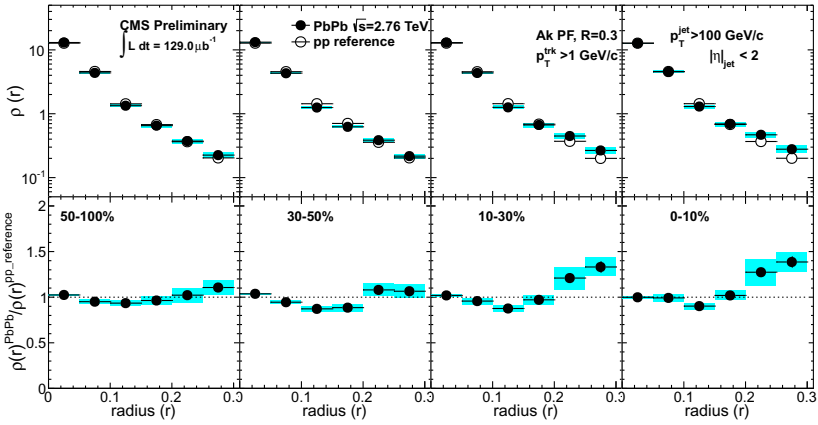

Figure 5: Differential jet shapes in PbPb and pp collisions are presented for different centrality bins for $p_{\mathrm{T}}^{jet} > 100$ GeV/c with track $p_{\mathrm{T}} > 1$ GeV/c (top panels). The background is subtracted by η reflection. Results from data are shown as black points while the open circles show the reference pp. In the bottom row, the ratio of the PbPb and pp jet shapes is shown. The blue band shows the total systematic while the error bars indicate the statistical errors.

of discriminators based on, e.g. the significance of the flight distance of the reconstructed secondary vertex with respect to the primary collision vertex. For the tagged jets, the fraction of b-jets can be obtained using fits of MC-based templates for, e.g., the secondary vertex mass.

The left panel of Fig. 4 shows the b-jet fraction as function of jet p_{T} for minimum bias 2.76 TeV PbPb collisions. The b-jet fraction is around 3% with no significant p_{T} dependence, consistent with PYTHIA predictions and the values observed in pp collisions at the same collision energy (right panel).

The b-jet fraction in PbPb collisions was also found to be independent of collision centrality. As a consequence, the data indicate that the b-jets in the p_{T} range have a nuclear suppression factor similar to that of inclusive jets, i.e. about 0.5 in central PbPb collisions.

5. Jet shapes and fragmentation functions

The study of the modification of jet shapes and fragmentation functions provides complementary information to measurements of jet energy loss using, e.g., jet R_{AA} or dijet imbalance. In CMS, the fragmentation properties of inclusive jets with $p_{\mathrm{T,jet}} > 100$ GeV/c in PbPb collisions are studied using differential jet shapes and fragmentation functions based on reconstructed charged particles. The PbPb results are compared to reference distributions based on pp data collected at the same collision energy, which take into account the additional resolution smearing seen in PbPb due to the underlying event fluctuations, as well as any differences in the jet-p_{T} spectral shape between PbPb and pp. The jet shapes and fragmentation functions are measured for reconstructed charged particles with $p_T > 1$ GeV/c within the jet cone. The differential jet shape is defined as the transverse momentum fraction, $\rho(r)$, carried by charged particles as a function of their distance $r = \sqrt{\Delta\eta^2 + \Delta\phi^2}$ from the jet axis.

In the Fig. 5, the differential jet shape results in PbPb are compared with the shapes obtained for the pp-based reference. The bottom panel presents the ratio of the jet shape between PbPb

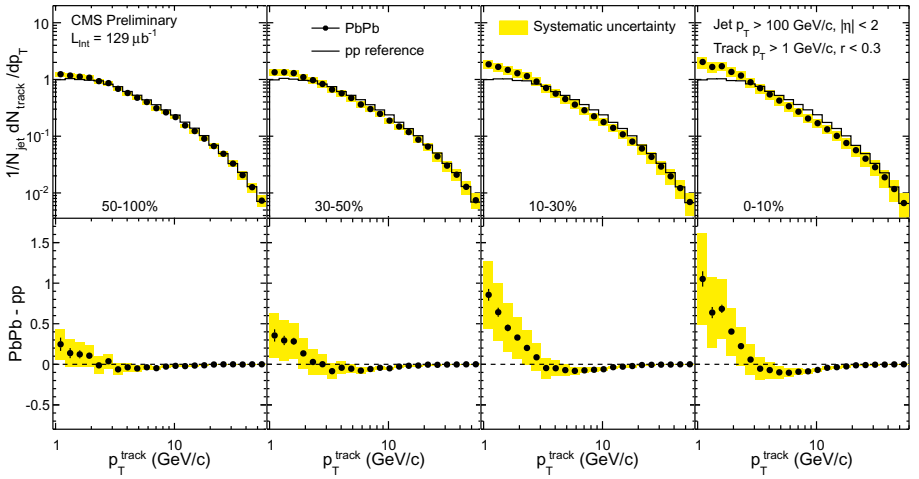

Figure 6: The spectrum of tracks inside the jet cone, as a function of track p_{T}, for PbPb and pp. Both the PbPb and pp results are background subtracted, in the same manner as the fragmentation functions. Bottom panel shows the difference of PbPb and pp spectra, which shows that there is an excess of low-p_{T} tracks in the PbPb events.

and pp for different centralities. The ratios are close to unity for mid-peripheral and peripheral collisions (30-50% and 50-100%), and show a rising trend towards large radius r for mid-central and central collisions (10–30% and 0–10%). Overall, the results indicate a moderate, but significant broadening of the jet structure in the central PbPb collisions, where a small fraction of the jet energy is transported from the core of the jet closer to the edge of the $R = 0.3$ jet cone.

The study of jet shapes is complemented by measurements of the jet fragmentation functions. These can be plotted in a variety of ways. In Fig. 6 we show the p_{T} spectra of charged particles in the jet cone, after background subtraction. In the lower row, the difference of the particle spectra between PbPb and the pp based reference is shown.

As for the jet-shapes analysis, the in-cone particle spectra for the peripheral data are in good agreement with the pp-based reference. For more central collisions however, a significant modification of the fragmentation properties in PbPb compared to pp in the intermediate and low p_{T} region develops. For p_{T} between 3 and about 20 GeV/c, i.e. in the intermediate p_{T} range of fragmentation products, a depletion in PbPb spectra compared to pp is seen, which is accompanied by an excess in the PbPb particle spectra for p_{T} of 1-3 GeV/c. In this representation of the fragmentation properties, the absolute amount of momentum transport can be readily quantified by integrating the excess seen in the PbPb vs. pp difference. For central events, this corresponds to less than 2% of the jet energy.

6. Quarkonium suppression

At this conference CMS has presented measurements in PbPb collisions at $\sqrt{s_{NN}} = 2.76$ TeV for prompt and non-prompt J/ψ [11], inclusive ψ' [9], and the three Υ states [12]. A striking illustration of the capabilities of CMS is shown in Fig. 7(left), which shows the invariant mass distribution of $\mu^+\mu^-$ pairs in the Υ mass region for minimum bias PbPb collisions. Also shown

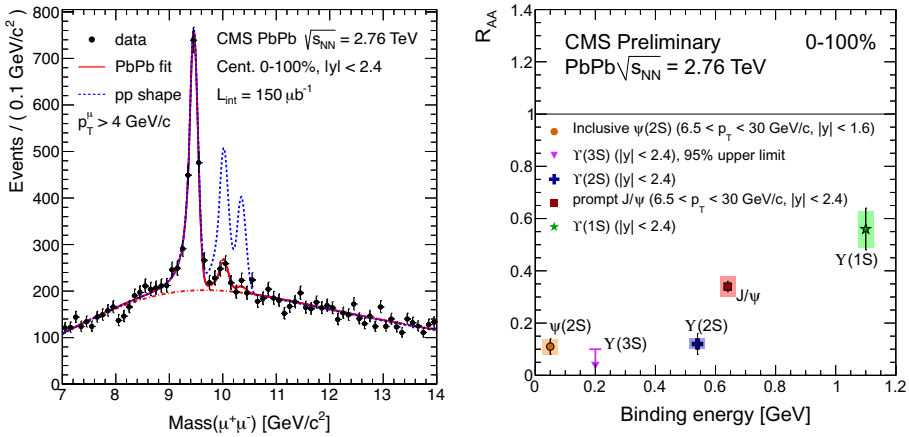

Figure 7: (Left): Dimuon invariant mass distribution in the ϒ mass region for minimum bias PbPb collisions. The dashed blue line shows the line shape obtained from a fit to the spectrum in pp collisions at the same collision energy, normalized to the ϒ(1S) peak. (Right): Minimum bias R_{AA} for all quarkonia states measured by CMS. For ϒ(3S) the upper limit (95% CL) is given. Points are from [9], [10], and [11].

is a fit to the mass distribution seen in pp collisions at the same collision energy as PbPb. The plot shows the clear separation of the ϒ(nS) mass states achieved by CMS in both pp and PbPb.

One of the long-standing goals in these studies is to use the dependence of the observed suppression factors on the binding energies of the various quarkonium states to constrain initial medium properties, e.g., in particular the initial temperature. The sequential suppression of the three ϒ(nS) states in the order of their binding energies is plainly visible in the comparison of the pp line shape and the PbPb data, following expectations for their dissolution in a hot QCD medium. The suppression relative to pp for the individual states was found to be about 2, 8, and larger than 10, for ϒ(1S), ϒ(2S) and ϒ(3S) respectively.The dependence is further quantified in Fig. 7(right), which shows the R_{AA} factors for the charmonium and bottomonium states in minimum bias PbPb collisions as a function of their binding energies. Although a detailed comparison will need to take the different p_T cuts for $c\bar{c}$ and $b\bar{b}$ states into account, the expected decrease of the suppression (i.e. increase in R_{AA}) is once again observed for states with increasing binding energy. Further experimental studies using data from a future pPb run at LHC will be necessary to understand the possible cold nuclear matter effects in the observed quarkonium suppression and to allow quantitative evaluation of the underlying medium properties.

7. Summary

Using the high statistics data set collected in 2011, CMS has greatly extended the p_T reach, precision and scope of measurements related to the key properties of the strongly interacting medium formed in heavy collisions. Ultra-central collisions provide a new testing ground for models of the initial state and the hydrodynamic expansion, while high-p_T anisotropy measurements characterize the path length dependence of parton energy loss. Earlier jet quenching measurements have been complemented by various studies of nuclear modification factors for unsuppressed probes such as Z^0's and W's, which provide a reference for the suppression seen in

inclusive jets and, for the first time, in b-tagged jets. The suppression of inclusive jets confirms the results seen in inclusive charged hadrons, and complements the information from high-p_{T} dijet imbalance measurements. Modifications to the jet fragmentation properties have been studied with jet shape and fragmentation function measurements, which demonstrate a moderate, but significant, modification of the radial and p_{T}-dependence of the energy flow within the jet cone in PbPb collisions compared to pp. Finally, high precision data on the sequential suppression of the Υ(nS) family and the charmonium family at $p_{\mathrm{T}} > 6.5$ GeV/c confirm the expected suppression pattern from Debye screening in the hot medium.

References

[1] S. Chatrchyan, et al., The CMS experiment at the CERN LHC, JINST 3 (2008) S08004. doi:10.1088/1748-0221/3/08/S08004.

[2] CMS, CMS Public Heavy Ion Results.
URL `https://twiki.cern.ch/twiki/bin/view/CMSPublic/PhysicsResultsHIN`

[3] B. Alver, G. Roland, Collision geometry fluctuations and triangular flow in heavy-ion collisions, Phys.Rev. C81 (2010) 054905. arXiv:1003.0194, doi:10.1103/PhysRevC.82.039903, 10.1103/PhysRevC.81.054905.

[4] M. Luzum, J.-Y. Ollitrault, Extracting the shear viscosity of the quark-gluon plasma from flow in ultra-central heavy-ion collisions (2012). arXiv:1210.6010.

[5] J. Jia, W. Horowitz, J. Liao, A study of the correlations between jet quenching observables at RHIC, Phys.Rev. C84 (2011) 034904. arXiv:1101.0290, doi:10.1103/PhysRevC.84.034904.

[6] B. Betz, M. Gyulassy, G. Torrieri, Fourier harmonics of high-p_T particles probing the fluctuating initial condition geometries in heavy-ion Collisions, Phys.Rev. C84 (2011) 024913. arXiv:1102.5416, doi:10.1103/PhysRevC.84.024913.

[7] CMS, Very high-p_{T} dihadron correlations in PbPb collisions at $\sqrt{s_{NN}}$= 2.76 TeV, CMS Physics Analysis Summary CMS-PAS-HIN-12-010 (2012).
URL `http://cdsweb.cern.ch/record/1472744`

[8] S. Chatrchyan, et al., Suppression of non-prompt J/ψ, prompt J/ψ and Υ in PbPb collisions at $\sqrt{s_{NN}}$= 2.76 TeV, JHEP 1205 (2012) 063. arXiv:1201.5069, doi:10.1007/JHEP05(2012)063.

[9] CMS, Measurement of the ψ(2S) meson in PbPb collisions at $\sqrt{s_{NN}}$= 2.76 TeV, CMS Physics Analysis Summary CMS-PAS-HIN-12-007 (2012).
URL `http://cdsweb.cern.ch/record/1455477`

[10] S. Chatrchyan, et al., Study of high-p$_T$ charged particle suppression in PbPb compared to pp collisions at $\sqrt{s_{NN}}$=2.76 TeV, Eur.Phys.J. C72 (2012) 1945. arXiv:1202.2554, doi:10.1140/epjc/s10052-012-1945-x.

[11] CMS, J/ψ results from CMS in PbPb collisions, with 150 μb^{-1}, CMS Physics Analysis Summary CMS-PAS-HIN-12-014 (2012).
URL `https://cdsweb.cern.ch/record/1472735`

[12] S. Chatrchyan, et al., Observation of sequential Υ suppression in PbPb collisions, accepted by Physics Review Letters (2012). arXiv:1208.2826.